ACS OMEGA

http://pubs.acs.org/journal/acsodf

Article

Preparation and Study on the Flame-Retardant Properties of CNTs/PMMA Microspheres

Lanjuan Xu, Juncheng Jiang,* Xinlei Jia, Yingying Hu, Lei Ni, Chao Li, and Wenjie Guo

Cite This: *ACS Omega* 2022, 7, 1347−1356

Read Online

ACCESS | Metrics & More | Article Recommendations

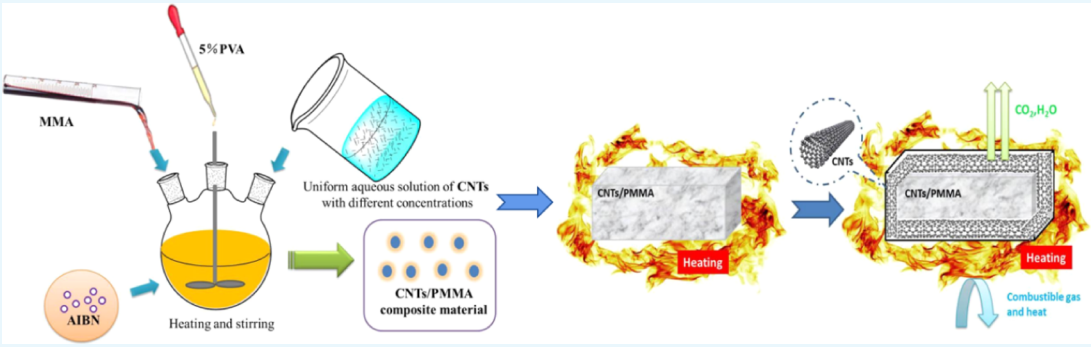

ABSTRACT: In this paper, carbon nanotubes (CNTs)/poly(methyl methacrylate) (PMMA) composites with excellent thermal stability and flame retardancy were prepared by in situ polymerization. The morphology, structure, transmittance, thermal stability, flame retardancy, and mechanical properties of the materials were characterized with scanning electron microscopy (SEM), thermogravimetric analysis (TGA), cone calorimetry, etc. According to the results, the initial decomposition temperature of CNTs/PMMA prepared using carbon nanotubes with a concentration of 2 mg/mL increases from 175 to 187 °C when compared with pure PMMA, and the weight loss ratio decreases significantly at the same time. In addition, the maximum limiting oxygen index (LOI) value of CNTs/PMMA composites is 22.17, which is 26.9% higher than that of PMMA. SEM images of residues after LOI tests demonstrate that when CNTs/PMMA is heated, a dense and stable interconnected network structure (i.e., carbon layer) is formed, which can effectively inhibit the combustion of pyrolysis products, prevent the transfer of heat and combustible gas, and finally interrupt the combustion of composite materials. However, a 25% decrease in the transmittance of CNTs/PMMA composites is observed in the Ultraviolet−visible (UV−vis) spectra. Although the addition of CNTs reduces the transparency of PMMA, its tensile and impact strength are all improved, which illustrates that CNT is a competitive flame retardant for PMMA.

1. INTRODUCTION

Poly(methyl methacrylate) (PMMA), also known as plexiglass, is characterized by high light transmittance, excellent optical performance, and easy processing. It is often used as a substitute for glass in aviation, construction, transportation, and other fields.[1,2] However, due to the poor fire resistance of PMMA, it is easy to cause melting and dripping during combustion, which can easily lead to the spread of fire.[3] As a result, the application of PMMA is limited. Therefore, the preparation of PMMA with excellent flame-retardant properties has become a research hotspot.

Laachachi[4] et al. incorporated ammonium polyphosphate (APP), Al_2O_3, and TiO_2 in PMMA. They found that both APP-based additives and oxide nanoparticles could improve the thermal stability and reduce the heat release rate (HRR) of PMMA, and they attribute these improvements to the catalytic effects of the oxide surface to modify the degradation pathway of PMMA and the formation of a charred and ceramized structure. Xie[5] et al. synthesized a phosphorus-containing acrylate monomer and introduced it into the PMMA matrix by in situ polymerization. After the modification, the limiting oxygen index (LOI) value of PMMA increased from 17.5 to 27.5%, and meanwhile, the peak HRR and total heat release (THR) were greatly reduced. Vahabi[6] et al. studied the thermal degradation and flame retardancy of PMMA containing different mineral fillers in combination with APP. The results showed that the combination of APP and sepiolite improved the fire behavior of PMMA significantly. Yang[7] et al. synthesized a novel PMMA-based copolymer (PMMA-co-

Received: October 25, 2021
Accepted: December 17, 2021
Published: December 28, 2021

BDPA) via radical copolymerization. The copolymer exhibited a 23% increase in the LOI value, and the PHRR of PMMA was reduced by 29.2%.

With the progress and development of modern nanotechnology, nano-flame-retardant materials have been highly developed. Among them, nanocarbon materials such as fullerene, graphene, and carbon nanotubes can improve flame retardancy and the mechanical property of polymers.[8−11] Dittrich[12] et al. prepared a polypropylene/multiwall carbon nanotube composite by melt blending and found that with the continuous addition of carbon nanotubes, the initial thermal decomposition temperature and maximum thermogravimetric temperature of the composite material system increased and the thermal stability was improved. Zuo[13] et al. prepared polyimide (PI) composite aerogels with enhanced flame-retardant properties using freeze-drying methods by adding environmentally friendly flame-retardant additives (i.e., graphene and montmorillonite), and it is found that there is a strong interaction between the two components, and the graphene oxide/MMT hybrid can be dispersed in water synergistically to enhance the mechanical properties, thermal stability, and flame retardancy of the composite aerogel. Cao[14] et al. used in situ polymerization to bond graphene oxide (GO) derivative (i.e., sheets and nanoribbons) coatings to the PDMS foam surface. It is interesting to find that the two GO derivatives can significantly improve the thermal stability and flame retardancy of PDMS foam without affecting its density and elasticity. Wu[15] et al. uniformly dispersed CNTs in a flame retardant, which not only enabled the composite material to exhibit good mechanical properties but also effectively improved the flame-retardant performance of the composite material, and its limiting oxygen index value could reach 25.5%. Three-dimensional flame-retardant carbon−carbon nanotube hybrid foam was prepared by Patle,[16] and he found that adding three-dimensional flame-retardant carbon−carbon nanotubes to phenolic resin not only increased its compressive strength (6.5 MPa) but also increased heat stability and flame retardancy.

However, nanocarbon materials generally have some defects, such as poor dispersion, easy agglomeration, low chemical activity, and poor compatibility with polymers. Therefore, functional monomers such as silane coupling agents and phosphorus-containing flame retardants can be introduced into nanocarbon materials to overcome these shortcomings.[17] Xing[18] et al. prepared functionalized carbon nanotubes (DPPA-MWCNT) with the reaction of aminated multiwalled carbon nanotubes and diphenylphosphinic chloride. The experimental results showed that DPPA-MWCNT nanofillers were more uniformly distributed within the PS matrix than unmodified carbon nanotubes. Therefore, the thermal stability, glass transition temperature, and tensile strength of PS/DPPA-MWCNT were greatly improved in comparison with PS/A-MWCNT. Xie[19] et al. synthesized a composite consisting of carbon nanotubes and zinc aluminum-layered double hydroxide (CNT/ZnAl-LDH) and analyzed its effect on the thermal stability and flammability performance of flexible polyurethane (PU) foams. According to the results, the maximum reduction of the peak HRR of PU/CNT/ZnAl-LDH foams was 13.5% compared with pure PU foam. Yang[20] et al. fabricated poly(lactic acid) (PLA) biocomposites using CaMg-Ph as a biosourced phosphorous additive combined with acid-treated carbon nanotubes and evaluated their thermal, mechanical, and flame-retardant properties. They found that PLA/CaMg-Ph19/CNT1 (1 wt % CNT and 19 wt % CaMg-Ph) showed lower PHRR (35.0%) and higher char yield (18.4 wt %) compared with PLA/CaMg-Ph20 (20 wt % CaMg-Ph) because of the reinforcement effect of CNTs.

In this paper, the in situ polymerization method was adopted to improve the flammability of poly(methyl methacrylate) (PMMA) by introducing carbon nanotubes (CNTs) with different concentrations, and a highly flame-retardant CNTs/PMMA composite material was prepared. The apparent morphology of PMMA and CNTs/PMMA microspheres was observed using an optical microscope and a scanning electron microscope, and their structure was analyzed using infrared spectroscopy. The thermal stability and flame-retardant properties were characterized. Finally, the effect of CNTs on the thermal stability and flame retardancy of PMMA and its mechanism were explored.

2. EXPERIMENT PART

2.1. Experimental Reagents. Methyl methacrylate (MMA, 99.5%), azobisisobutyronitrile (AIBN, 98%), and multiwalled carbon nanotubes (CNTs, 90%) were provided by Shanghai Maclean Biochemical Technology Co., Ltd. Poly(vinyl alcohol) (PVA, analytical grade) was purchased from Shanghai Aladdin Biochemical Technology Co., Ltd. Tetrahydrofuran (analytical purity), absolute ethanol (95%), potassium hydroxide (KOH, 95%), and potassium persulfate (KPS, 99%) were obtained from Tianjin Tianli Chemical Reagent Co., Ltd.

2.2. Experimental Equipment and Instruments. The oxygen index tester (SH5706A) was obtained from Guangzhou Xinhe Electronic Equipment Co., Ltd. The optical microscope (N-180M) was provided by OLYMPUS, Japan. The desktop low-speed centrifuge (TDL-5) was purchased from Jintan Liangyou Experimental Instrument Factory. A synchronous thermal analyzer (STA449F3) and a Fourier exchange infrared spectrometer (Nicolet 380) were provided by the German company, Netzsch. The cone calorimeter (FTT Standard Cone Calorimeter) was provided by Fire Testing Technology Limited, the U.K. The UV/NIR spectrophotometer (Lambda75) was purchased from Shanghai Changfang Optical Instrument Co., Ltd. The electronic universal testing machine (WDW 50M) was purchased from Jinan Zhongluchang Testing Machine Manufacturing Co., Ltd.

2.3. Preparation of CNTs/PMMA Composite Material.

(1) Preparation of dispersant: 5.26 g of flocculent poly(vinyl alcohol) (PVA) was weighed and added to 100 mL of distilled water and stirred for 12 h. The reaction temperature started from 50 °C, and each unit was stirred for 2 h. The 5% PVA solution was successfully prepared when it was observed that the solution in the flask was uniformly mixed, transparent, and free of impurities.

(2) Preparation of PMMA microspheres: briefly, 0.5 g of 5% PVA solution was dropped into a three-necked flask filled with 40 mL of distilled water. After stirring the solution at 320 rpm for 5 min at a temperature of 40 °C, 6 mL of methyl methacrylate (MMA) solution was added, the temperature was gradually increased, and a small amount of AIBN was added at 50, 60, and 70 °C. Then, the temperature was slowly increased to 78 °C and reacted for 90 min. A small number of beads were taken out from the flask with a disposable plastic

https://doi.org/10.1021/acsomega.1c05606
ACS Omega 2022, 7, 1347−1356

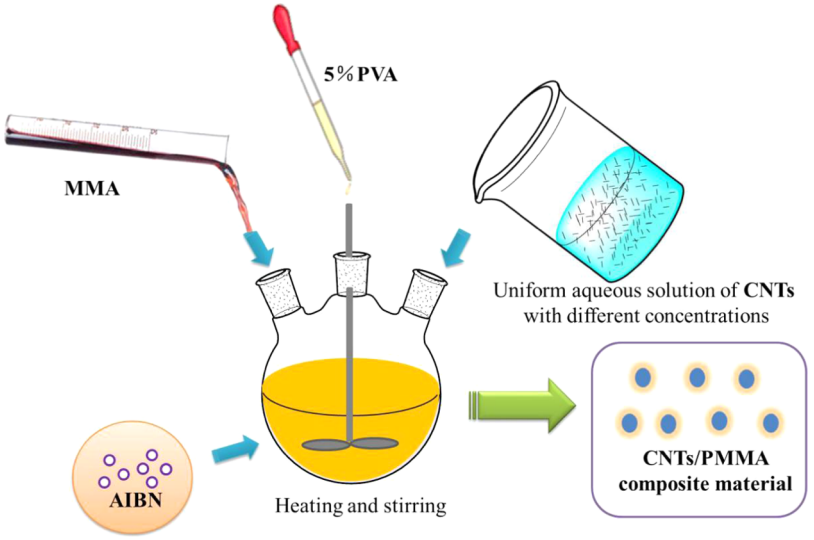

Figure 1. Preparation diagram of the CNTs/PMMA composite.

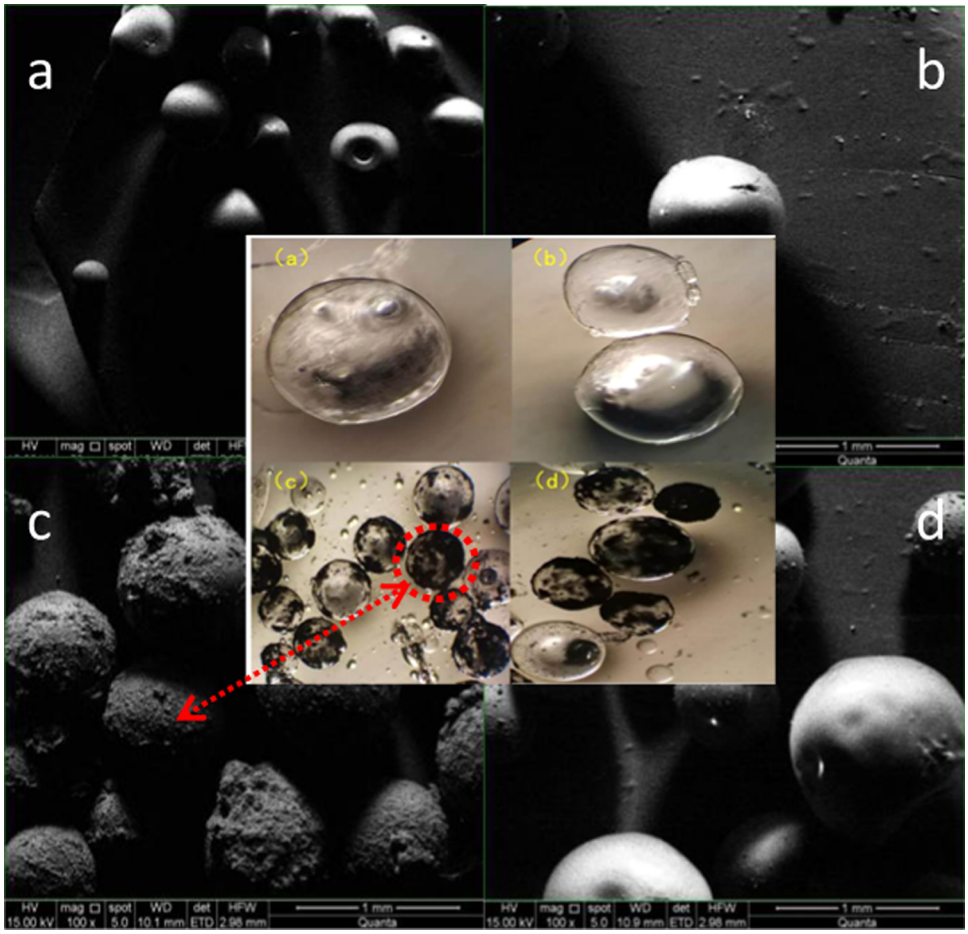

Figure 2. Scanning electron microscopy image of the composite material. (a) PMMA material, (b) 0.5 mg/mL CNTs/PMMA composite material, (c) 1 mg/mL CNTs/PMMA composite material, and (d) 1.5 mg/mL CNTs/PMMA composite material.

dropper and dropped into distilled water to see if they harden and settle. If they become hard, the temperature and rotation speed are increased appropriately to accelerate the formation of the beads. If they do not become hard, the reaction is continued for 10 min. After the reaction ends, PMMA microspheres were successfully prepared.

(3) Preparation of carbon oxide nanotubes: quantitative multiwalled carbon nanotubes and 300 mL of distilled water were placed in a flask and ultrasonically shaken and dispersed for 3 h. Then, 2.7 g of potassium persulfate (KPS) was added into a beaker, and a KOH solution with a concentration of 1 mol/L was added to adjust the pH value of the reaction system to 13. The

https://doi.org/10.1021/acsomega.1c05606
ACS Omega 2022, 7, 1347−1356

mixture was poured into a flask equipped with a condensing reflux tube, stirred vigorously in a water bath at 85 °C for 5 h, and cooled to room temperature naturally. Then, it was centrifuged at 3000 rpm for 5 min and washed repeatedly with distilled water. Finally, the product was dried at a temperature of 60 °C for 24 h.

(4) CNTs/PMMA composite material preparation: the oxidized carbon nanotubes were configured into 0.5, 1, and 2 mg/mL solutions and ultrasonically vibrated for 1 h to obtain a uniform solution. The distilled water used in the PMMA preparation process in step (1) was replaced with different concentrations of oxidized water. A homogeneous aqueous solution of carbon nanotubes, and then in accordance with the experimental process of the preparation step (1), CNTs/PMMA composite material was successfully prepared. Finally, the product was filtered and dried to obtain the CNTs/PMMA composite material. The preparation diagram of the CNTs/PMMA composite is shown in Figure 1.

3. RESULTS AND DISCUSSION

3.1. Morphology Analysis of the CNTs/PMMA Composite. The morphology of PMMA and CNTs/PMMA composites was observed using optical microscopy (OM) and scanning electron microscopy (SEM), and the influence of the addition of CNTs on the appearance and structure of PMMA was analyzed. The result is shown in Figure 2.

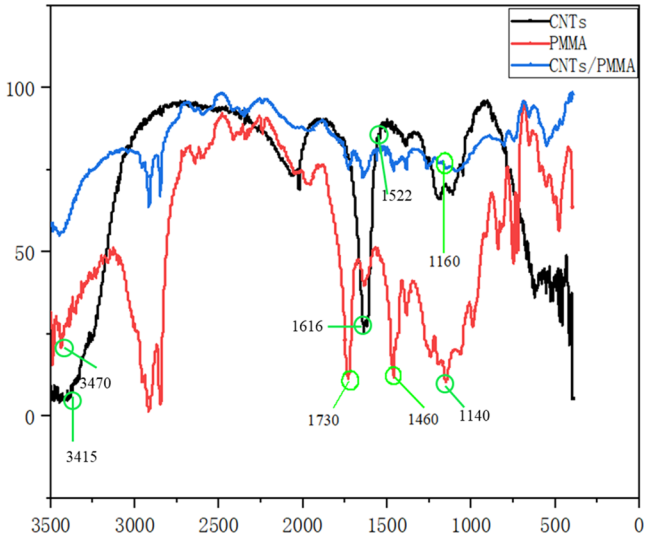

Figure 3. Fourier infrared spectrum of composite materials.

As shown in Figure 2a, the PMMA materials present an obvious spherical structure and good light transmittance, but the surface is slightly convex, and there are small bubbles in the microspheres. It can be clearly seen that there is a lot of black powdery substance attached to the surface of the smooth PMMA microspheres, which means that CNTs have been successfully attached to PMMA and the CNTs/PMMA composite has been successfully prepared. As shown in Figure 2b, the surface of the CNTs/PMMA composite prepared with 0.5 mg/mL CNT solution is basically similar to the surface of pure PMMA. This may be due to the less addition of CNTs, and the effect on PMMA is not obvious. Interestingly, on the surface of the CNTs/PMMA composite with a CNT concentration of 1 mg/mL, there are a large number of fluffy protrusions, as shown in Figure 2c, indicating that CNTs have

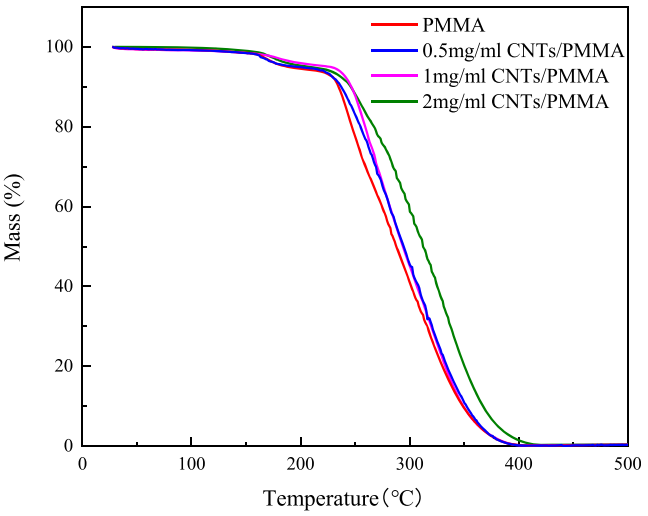

Figure 4. TGA curves of composite materials.

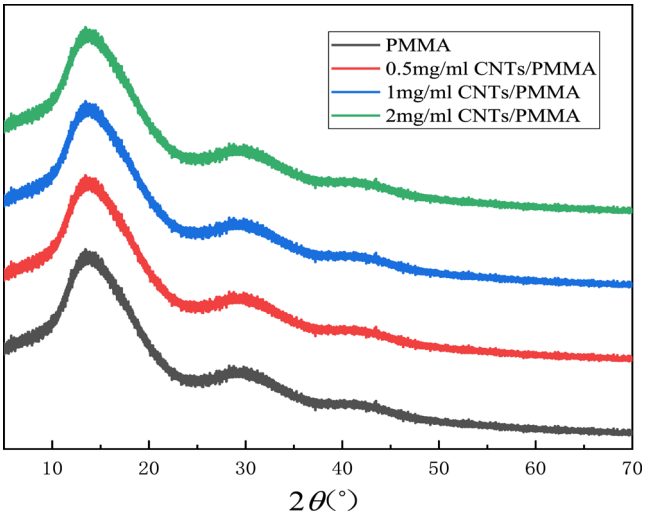

Figure 5. X-ray diffraction curves of composite materials.

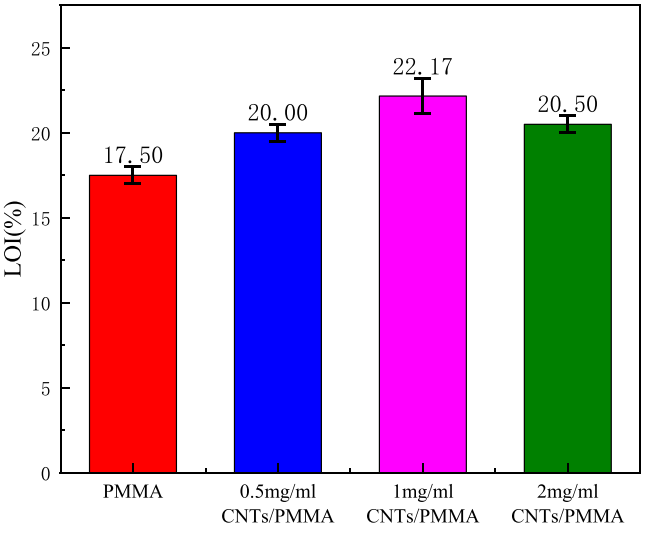

Figure 6. Limiting oxygen index of composite materials.

https://doi.org/10.1021/acsomega.1c05606
ACS Omega 2022, 7, 1347−1356

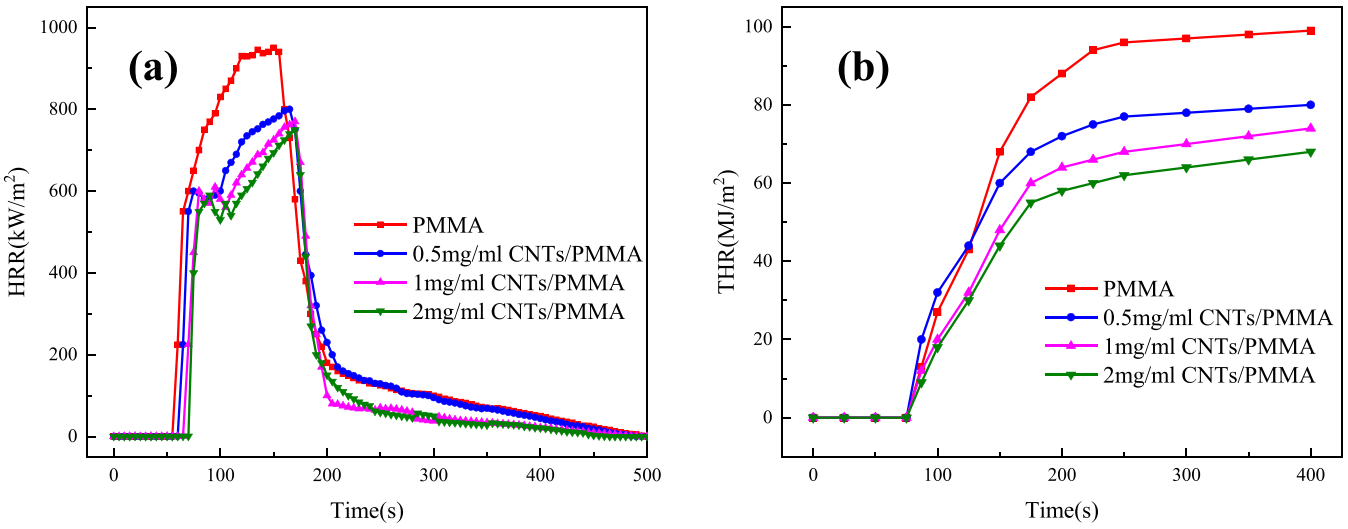

Figure 7. (a) HRR and (b) THR curves of composite materials.

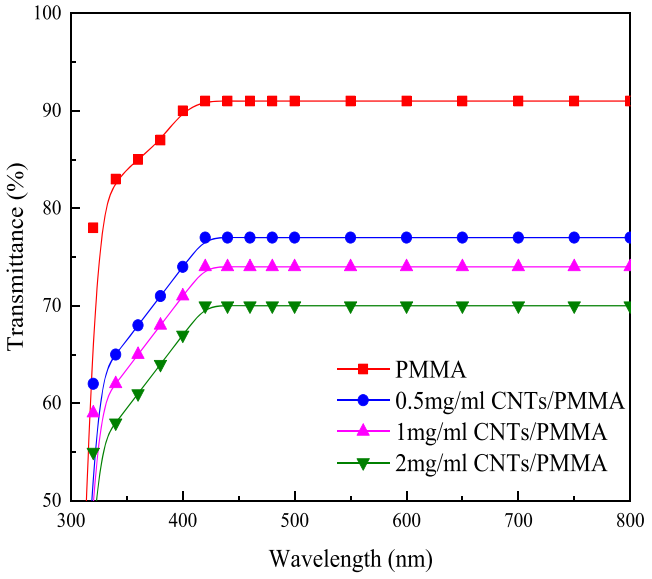

Figure 8. Ultraviolet−visible (UV−vis) spectroscopy spectra of composite materials.

been uniformly attached to the PMMA, and the CNTs/PMMA composite has been successfully prepared. However, as shown in Figure 2d, the surface of the 2 mg/mL CNTs/PMMA composite is relatively smooth, with small fluffy protrusions attached, and a small number of CNTs are adsorbed on PMMA. This shows that with the increase of the CNT content, the number of CNTs attached to the surface of PMMA microspheres decreases, which may be caused by the agglomeration of CNTs during the preparation process. On the whole, the adhesion of CNTs with a concentration of 1 mg/mL is the best.

3.2. Fourier Transform Infrared (FT-IR) Spectroscopy Analysis. To prove that the free radical in situ polymerization reaction occurred between CNTs and PMMA, the Fourier infrared spectrum of CNTs, PMMA, and CNTs/PMMA are compared in Figure 3.

As shown in Figure 3, the C═O ester group absorption peak at 1730 cm^{-1}; the C−H bending vibration absorption peaks at 1460, 1327, and 1160cm^{-1}; and the stretching vibration peak of the C−O−C group at 1140 cm^{-1} are the characteristic absorption peaks of PMMA, and CNTs have a stretching vibration peak of −C═C− at 1522 cm^{-1}. It is worth noting that because many characteristic oxygen-containing groups appear during the oxidation process of CNTs, they result in peaks such as the hydroxyl stretching vibration characteristic peak at 3415 cm^{-1} and the −C═O− stretching vibration characteristic peak at 1616 cm^{-1}. Interestingly, it can be seen that the infrared spectrum curve shape of the CNTs/PMMA composite material is similar to that of PMMA, indicating that PMMA is the main body in the composite material. We are surprised to find that the CNTs/PMMA composites have both the characteristic strong peaks of PMMA and those of CNTs, indicating that CNTs/PMMA composites have been successfully prepared.

3.3. Thermogravimetric Analysis (TGA). The thermal weight loss curves of CNTs/PMMA composites prepared from CNTs with different contents (0.5, 1.0, and 2.0 mg/mL) are shown in Figure 4. By comparing the TGA curves, the effect of different concentrations of CNTs on the thermal stability of PMMA composites is studied.

As shown in Figure 4, the initial decomposition temperature of pure PMMA is 175 °C, and there is almost no residue when heated to 400 °C, which shows that PMMA decomposes completely after heating. Due to the small content of CNTs, the thermogravimetric curve of 0.5 mg/mL CNTs/PMMA is similar to that of pure PMMA. However, with an increase of the CNT content, the initial decomposition temperature of 1.0 and 2.0 mg/mL CNTs/PMMA increased to 187 °C. In addition, the thermogravimetric rate of 2.0 mg/mL CNTs/PMMA is significantly decreased, and there are still some residues after thermal pyrolysis of the composites. Therefore, it can be concluded that the addition of CNTs can increase the initial thermal decomposition temperature and improve the thermal stability of PMMA. This is because CNTs can prevent both the further decomposition of PMMA and the entry of internal thermal decomposition products into the gas phase and their participation in combustion.

3.4. X-ray Diffraction (XRD) Analysis. The X-ray diffraction curves of PMMA and CNTs/PMMA composites are shown in Figure 5.

https://doi.org/10.1021/acsomega.1c05606
ACS Omega 2022, 7, 1347−1356

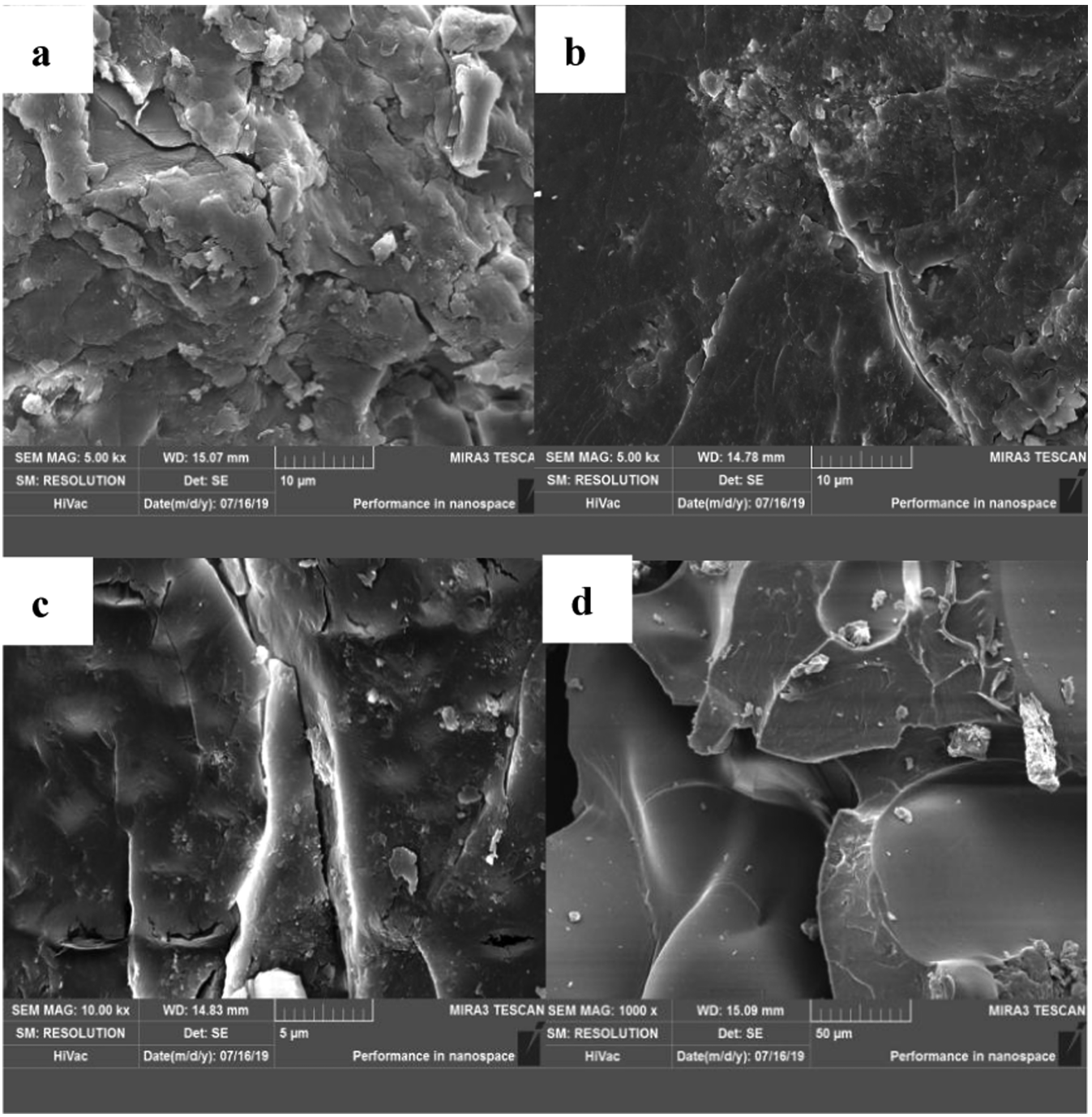

Figure 9. SEM images of samples after the LOI test. (a) PMMA, (b) 0.5 mg/mL CNTs/PMMA, (c) 1 mg/mL CNTs/PMMA, and (d) 2mg/mL CNTs/PMMA.

It can be observed from Figure 5 that both PMMA and CNTs/PMMA composites have obvious diffraction peaks at 2θ = 13.8, 29.3, and 41.4°. Moreover, the shape and position of the peaks are not significantly different. This may be due to the low addition of CNTs; it cannot significantly affect the crystalline structure of PMMA, which proves that after the addition of CNTs, the original performance of PMMA is not damaged. Since the wide and sharp diffraction peaks of the samples can be observed in Figure 5, we can conclude that the CNTs/PMMA composite has small crystal grains and good crystal shape.

3.5. Flame-Retardant Performance Analysis. The limiting oxygen index (LOI) of the sample was measured using an SH5706A oxygen index tester to analyze the minimum concentration of oxygen required for the combustion of PMMA and CNTs/PMMA composites. Three standard samples of PMMA, 0.5 mg/mL CNTs/PMMA, 1 mg/mL CNTs/PMMA, and 2mg/mL CNTs/PMMA were tested, respectively, and the average value of the limiting oxygen index was calculated. The results are shown in Figure 6.

According to Figure 6, the average LOI of pure PMMA is 17.50, and the LOI of 0.5 mg/mL CNTs/PMMA, 1 mg/mL CNTs/PMMA, and 2mg/mL CNTs/PMMA is 20.00, 22.17,

https://doi.org/10.1021/acsomega.1c05606
ACS Omega 2022, 7, 1347−1356

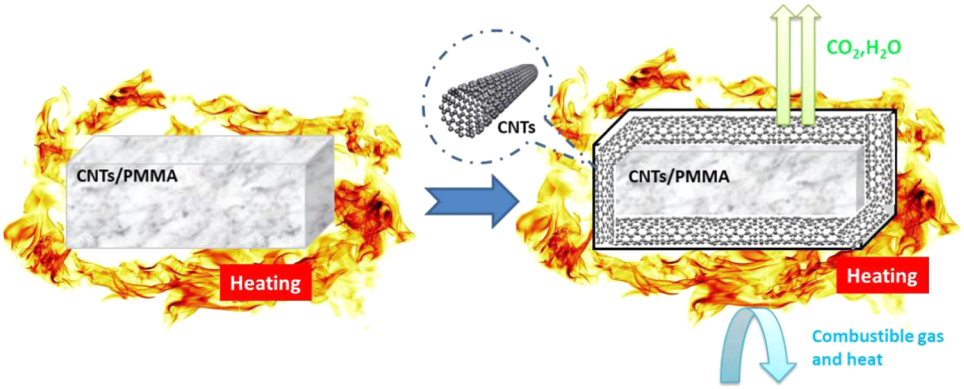

Figure 10. Flame-retardant mechanism diagram.

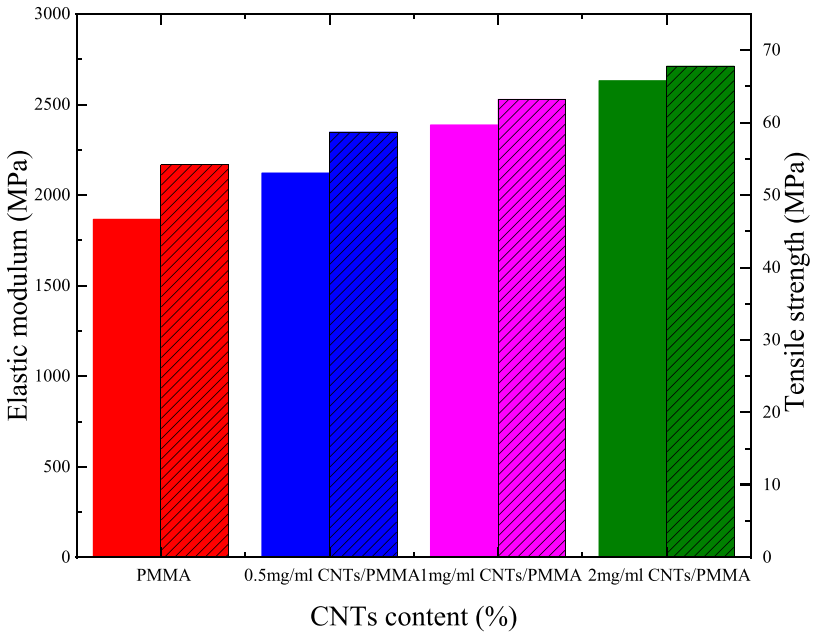

Figure 11. Elastic modulus and tensile strength of composite materials (the one with the diagonal pattern is tensile strength and the other is elastic modulus).

and 20.50, which is 14.3, 26.9, and 17.1% higher than that of PMMA, respectively. This shows that the addition of CNTs can indeed improve the flame retardancy of PMMA. However, it is interesting that the limiting oxygen index of the composite does not increase linearly with the increase of the amount of CNTs; this may be due to the agglomeration of CNTs when the content is too large, which affects their dispersion.

The excellent carbonization effect can not only improve the stability of polymer materials but also improve the flame-retardant properties of materials. Heat release rate (HRR) and total heat release (THR) are two important parameters to evaluate the fire hazards of polymers. The HRR curves of pure PMMA and the other three CNTs/PMMA composites are shown in Figure 7a. It can be seen that when the concentration of CNTs is 0.5mL/mg, the peak heat release rate (PHRR) is 796.7 kW/m^2, and the peak heat release rate of CNTs/PMMA decreases significantly with the addition of CNTs. Compared with 951.2 kW/m^2 of pure PMMA, the introduction of CNTs can reduce the peak heat release rate up to 201.5 kW/m^2. This shows that CNTs can effectively improve the flame-retardant performance of PMMA. This is because the mesh-structure carbon nanotubes form a relatively stable interconnected network on the surface of the composites, which affects the heat transfer in PMMA, and then improves the flame-retardant performance of CNTs/PMMA.

THR refers to the total heat released by polymers from ignition to extinction. As shown in Figure 7b, the maximum heat release of pure PMMA can be as high as 99.5 MJ/m^2. With the increase of the CNT content, THR of the composites gradually decreases. When 2 mg/mL CNT is added, the THR decreases to 69.3 MJ/m^2, which is 30.4% lower than that of pure PMMA. This shows that the addition of flame-retardant monomer CNTs can effectively reduce the total heat released during combustion and then prevent the heat from further promoting the combustion of PMMA.

3.6. Transmittance Analysis. The UV/NIR spectra were measured to evaluate the effect of CNTs on the transmittance of PMMA. Figure 8 shows the UV−vis spectra of pure PMMA and CNTs/PMMA composites. It can be seen that the transmittance of pure PMMA is 91% within the visible wavelength range (420−780 nm). With the increase of CNT addition, the transmittance of CNTs/PMMA within the visible wavelength range decreases. Compared with pure PMMA, the maximum decrease is about 25% (2 mg/mL CNTs/PMMA).

https://doi.org/10.1021/acsomega.1c05606
ACS Omega 2022, 7, 1347−1356

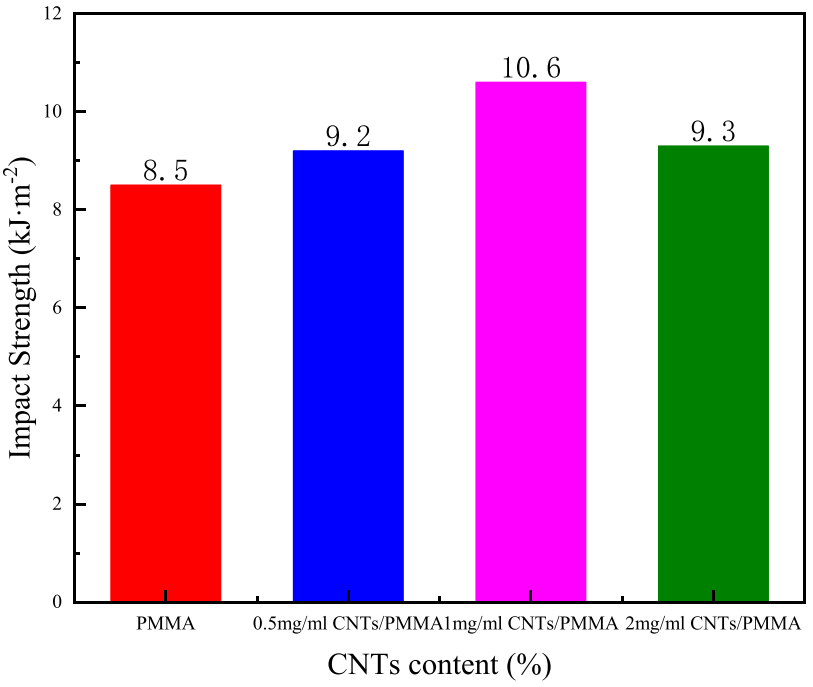

Figure 12. Impact strength of composite materials.

3.7. Analysis of the Flame-Retardant Mechanism. The flame-retardant mechanism in the condensed phase was analyzed according to the SEM images of residues after the LOI test, as shown in Figure 9.

It can be seen from Figure 9 that the surface of PMMA after combustion is relatively loose (Figure 9a), but the surfaces of burnt CNTs/PMMA composites become more and more compact with the increase of the CNT content (Figure 9b–d). The SEM images also show that there is a dense carbon layer generated by CNTs, which effectively hinders further combustion of the material. This result is consistent with that of the HRR analysis. Furthermore, the addition of CNTs significantly increases the melt viscosity of the composite; thus, the dripping of molten materials during combustion is effectively inhibited.

Besides the condensed phase, CNTs also work on the gas phase, as shown in Figure 10. When the composite material was heated, CNTs could quickly act on the active free radicals required for the branching reaction and generate inert gases such as CO_2 and H_2O, which can dilute the combustible gas to a certain extent, as well as absorb radiant heat and reduce the surface temperature of PMMA, thereby slowing down the violent combustion of the material.[21,22] At the same time, CNTs can form a dense and stable interconnected network structure (i.e., carbon layer)[23−26] on the surface, which can effectively inhibit the combustion of polymer cracked products and prevent the transfer of heat, combustible gas, etc., and finally combustion of the composite material.

3.8. Analysis of Mechanical Properties. Figure 11 shows the elastic modulus and tensile strength of CNTs/PMMA composites. It can be seen that the tensile strength and elastic modulus of pure PMMA are 54.2 and 1865.3 MPa, respectively. With the increase of CNT addition, both tensile strength and elastic modulus of the composites increase. Among them, the strength and elastic modulus of CNTs/PMMA composite prepared with 0.2 mg/mL CNTs are the highest (67.8 and 2630.1 MPa), which is increased by 24 and 41% when compared with pure PMMA, respectively. This is related to the network structure of CNTs in the PMMA matrix and the interface between them. CNTs have ultrahigh heterogeneous nucleation ability, which is conducive to the crystallization of PMMA on their surface, resulting in strong interfacial adhesion between them. When CNTs are dispersed well in the PMMA matrix, they form a network structure, which can improve the interaction with molecular chains. The molecular chains do not slip easily; therefore, they can withstand greater stress and improve the elastic modulus and tensile strength of the composites.

To further explore the effect of CNTs on the toughness of PMMA, the impact strength was tested. Figure 12 shows the non-notched impact strength of PMMA and CNTs/PMMA composites. It can be seen from Figure 12 that the non-notched impact strength of CNTs/PMMA increases first and then decreases. Compared with pure PMMA, the impact strength of 1 mg/mL CNTs/PMMA increases by 25%. This is because CNTs are well dispersed in the matrix and their interfacial adhesion and energy absorption effects are relatively good under this condition; therefore, the impact resistance is improved. However, with the increase of the CNT content, the dispersion of CNTs becomes worse, leading to local agglomeration which concentrates the stress and weakens the absorption of impact energy; therefore, the impact strength decreases (2 mg/mL CNTs/PMMA).

4. CONCLUSIONS

Using an in situ polymerization method, carbon nanotubes (CNTs) were innovatively introduced to improve the flammability of poly(methyl methacrylate) (PMMA), and a highly flame-retardant CNTs/PMMA composite with regular shape and uniform particle size distribution was prepared. The results show that the initial thermal decomposition temperature of the 2 mg/mL CNTs/PMMA composite material is 12 °C higher than that of PMMA, the corresponding weight loss ratio is smaller, and the thermal stability is better. In addition,

https://doi.org/10.1021/acsomega.1c05606
ACS Omega 2022, 7, 1347−1356

the PHRR and THR values of CNTs/PMMA composites decrease significantly compared with those of pure PMMA. On analyzing the flame-retardant mechanism of the condensed phase, it is found that CNTs can form a dense and stable interconnected network structure (i.e., carbon layer), which can effectively block the transmission of heat, combustible gas, etc., and thereby improve the flame retardancy of PMMA. Although the transmittance of PMMA is reduced slightly after the addition of CNTs, other properties of the composites such as thermal stability, flame retardancy, tensile strength, and impact strength are all improved, which makes CNT an effective flame retardant for PMMA.

AUTHOR INFORMATION

Corresponding Author

Juncheng Jiang − *College of Safety Science and Engineering, Nanjing Tech University, Nanjing, Jiangsu 210009, China; School of Environment and Safety Engineering, Changzhou University, Changzhou, Jiangsu 213164, China;* orcid.org/0000-0001-7018-2709; Email: jcjiang_njtech@163.com

Authors

Lanjuan Xu − *College of Safety Science and Engineering, Nanjing Tech University, Nanjing, Jiangsu 210009, China; College of Chemical Engineering and Safety, Binzhou University, Binzhou, Shandong 256600, China;* orcid.org/0000-0001-5191-0678

Xinlei Jia − *College of Chemical Engineering and Safety, Binzhou University, Binzhou, Shandong 256600, China*

Yingying Hu − *College of Chemical Engineering and Safety, Binzhou University, Binzhou, Shandong 256600, China*

Lei Ni − *College of Safety Science and Engineering, Nanjing Tech University, Nanjing, Jiangsu 210009, China;* orcid.org/0000-0001-5941-6156

Chao Li − *College of Safety Science and Engineering, Nanjing Tech University, Nanjing, Jiangsu 210009, China; College of Chemical Engineering and Safety, Binzhou University, Binzhou, Shandong 256600, China*

Wenjie Guo − *College of Safety Science and Engineering, Nanjing Tech University, Nanjing, Jiangsu 210009, China; College of Chemical Engineering and Safety, Binzhou University, Binzhou, Shandong 256600, China*

Complete contact information is available at: https://pubs.acs.org/10.1021/acsomega.1c05606

Notes

The authors declare no competing financial interest.

ACKNOWLEDGMENTS

The authors are grateful for the reviewers' instructive suggestions and careful proofreading. This work was supported by the National Natural Science Foundation of China (Nos. 51834007 and 21927815) and the Scientific Research Foundation of Binzhou University (No. BZXYLG1913).

REFERENCES

(1) Wang, W. S.; Liang, C. K.; Chen, Y. C.; Su, Y. L.; Tsai, T. Y.; Chen-Yang, Y. W. Transparent and flame retardant PMMA/clay nanocomposites prepared with dual modified organoclay. *Polym. Adv. Technol.* **2012**, *23*, 625−631.

(2) Fraser, R. A.; Stoeffler, K.; Ashrafi, B.; Zhang, Y.; Simard, B. Large-Scale Production of PMMA/SWCNT Composites Based on SWCNT Modified with PMMA. *ACS Appl. Mater. Interfaces* **2012**, *4*, 1990−1997.

(3) Kim, S.; Wilkie, C. A. Transparent and flame retardant PMMA nanocomposites. *Polym. Adv. Technol.* **2008**, *19*, 496−506.

(4) Laachachi, A.; Cochez, M.; Leroy, E.; Gaudon, P.; Ferriol, M.; Cuesta, J. M. L. Effect of Al2O3 and TiO2 nanoparticles and APP on thermal stability and flame retardance of PMMA. *Polym. Adv. Technol.* **2006**, *17*, 327−334.

(5) Xie, W.; Wang, B.; Liu, Y.; Wang, Q.; Yang, Z. Flame retardancy of a novel high transparent poly(methyl methacrylate) modified with phosphorus-containing compound. *React. Funct. Polym.* **2020**, *153*, No. 104631.

(6) Vahabi, H.; Lin, Q.; Vagner, C.; Cochez, M.; Ferriol, M.; Laheurte, P. Investigation of thermal stability and flammability of poly(methyl methacrylate) composites by combination of app with ZrO2, sepiolite or MMT. *Polym. Degrad. Stab.* **2016**, *124*, 60−67.

(7) Yang, B.; Wang, L.; Guo, Y.; Zhang, Y.; Tian, L.; et al. Synthesis of a novel phosphate-containing highly transparent PMMA copolymer with enhanced thermal and flame retardant properties. *Polym. Adv. Technol.* **2019**, *31*, 1−10.

(8) Rao, W. H.; Liao, W.; Wang, H.; Zhao, H. B.; Zhang, Y. Flame-retardant and smoke- suppressant flexible polyurethane foams based on reactive phosphorus-containing polyol and expandable graphite. *J. Hazard. Mater.* **2018**, *360*, 651−660.

(9) Zhu, Z.-M.; Rao, W. H.; Kang, A. H.; Liao, W.; Wang, Y. Z. Highly effective flame retarded polystyrene by synergistic effects between expandable graphite and aluminum hypophosphite. *Polym. Degrad. Stab.* **2018**, *154*, 1−9.

(10) Kashiwagi, T.; Du, F.; Winey, K. I.; Groth, K. M.; Shields, J. R.; Bellayer, S. P.; Kim, H.; Douglas, J. F. Flammability properties of polymer nanocomposites with single-walled carbon nanotubes effects of nanotube dispersion and concentration. *Polymer* **2005**, *46*, 471−481.

(11) Yuan, H.; Xiong, Y. L.; Luo, G. Q.; et al. Microstructure and electrical conductivity of CNTs/PMMA nanocomposite foams foaming by supercritical carbon dioxide. *J. Wuhan Univ. Technol., Mater. Sci. Ed.* **2016**, *31*, 481−486.

(12) Dittrich, B.; Wartig, K. A.; Hofmann, D.; Mülhaupt, R.; Schartel, B. Flame retardancy through carbon nanomaterials:Carbon biack,multiwall nanotubes,expanded graphite,multi-layer graphene and graphene in polypropylene. *Polym. Degrad. Stab.* **2013**, *98*, 1495−1505.

(13) Zuo, L.; Fan, W.; Zhang, Y.; Zhang, L.; Gao, W.; Huang, Y.; Liu, T. Graphene/montmorillonite hybrid synergistically reinforced polyimide composite aerogels with enhanced flame-retardant performance. *Compos. Sci. Technol.* **2017**, *139*, 57−63.

(14) Cao, C. F.; Wang, P. H.; Zhang, J. W.; Guo, K. Y.; Yang, L.; Xia, Q. Q.; Zhang, G. D.; Zhao, L.; Chen, H.; Wang, L.; et al. One-step and green synthesis of lightweight, mechanically flexible and flame-retardant polydimethylsiloxane foam nanocomposites via surface-assembling ultralow content of graphene derivative. *Chem. Eng. J.* **2020**, *393*, 124724−124760.

(15) Wu, Z.; Wang, H.; Tian, X.; Ding, X.; Xue, M.; Zhou, H.; Zheng, K. Mechanical and flame-retardant properties of styrene-ethylene-butylene-styrene/carbon nanotube composites containing bisphenol A bis(diphenyl phosphate). *Compos. Sci. Technol.* **2013**, *82*, 8−14.

(16) Patle, V. K.; Kumar, R.; Sharma, A.; Dwivedi, N.; Muchhala, D.; Chaudhary, A.; Mehta, Y.; Mondal, D. P.; Srivastava, A. K. Three dimension phenolic resin derived carbon-cnts hybrid foam for fire retardant and effective electromagnetic interference shielding. *Composites, Part C* **2020**, *2*, 100020−100030.

(17) Zhu, S.-E.; Wang, L. L.; Hao, C.; Wei, Y.; Anthony, Y.; Chen, T.; Cheng, L.; Bi, W. M.; Hu, E. Z.; Jian, Z.; et al. Comparative studies on thermal, mechanical, and flame retardant properties of PBT nanocomposites via different oxidation state phosphorus-containing agents modified amino-CNTs. *Nanomater.* **2018**, *8*, 70.

(18) Xing, W.; Yang, W.; Yang, W.; Hu, Q.; Si, J.; Lu, H.; Tang, B.; Song, L.; Hu, Y.; Yuen, R. K. K. Functionalized carbon nanotubes

with phosphorus and nitrogen-containing agents: effective reinforcer for thermal, mechanical, and flame-retardant properties of polystyrene nanocomposites. *ACS Appl. Mater. Interfaces* **2016**, *8*, 26266−26274.
(19) Xie, H.; Ye, Q.; Si, J.; Yang, W.; Lu, H.; Zhang, Q. Synthesis of a carbon nanotubes/ZnAl-layered double hydroxide composite as a novel flame retardant for flexible polyurethane foams. *Polym. Adv. Technol.* **2016**, *27*, 651−656.
(20) Yang, W.; Tawiah, B.; Yu, C.; Qian, Y. F.; Wang, L. L.; Yuen, A. C. Y.; Zhu, S. E.; Chen, T. B. Y.; Yu, B.; Lu, H. D.; et al. Manufacturing, mechanical and flame retardant properties of poly(lactic acid) biocomposites based on calcium magnesium phytate and carbon nanotubes. *Composites, Part A* **2018**, *110*, 227−236.
(21) Schartel, B.; Potschke, P.; Knoll, U.; Abdelgoad, M. Fire behaviour of polyamide 6/multiwall carbon nanotube nanocomposites. *Eur. Polym. J.* **2005**, *41*, 1061−1070.
(22) Shabestari, M. E.; Kalali, E. N.; González, V. J.; Wang, D. Y.; Fernández-Blázquez, J. P.; Baselga, J.; Martin, O. Effect of nitrogen and oxygen doped carbon nanotubes on flammability of epoxy nanocomposites. *Carbon* **2017**, *121*, 193−200.
(23) Im, J. S.; Lee, S. K.; In, S. J.; Lee, Y. S. Improved flame retardant properties of epoxy resin by fluorinated MMT/MWCNT additives. *J. Anal. Appl. Pyrolysis* **2010**, *89*, 225−232.
(24) Wang, N.; Li, L.; Xu, Y.; Zhang, K.; Chen, X.; Wu, H. Synergistic effects of red phosphorus masterbatch with expandable graphite on the flammability and thermal stability of polypropylene/thermoplastic polyurethane blends. *Polym. Polym. Compos.* **2020**, *28*, 209−219.
(25) Abdalla, M.; Dean, D.; Theodore, M.; Fielding, J.; Nyairo, E.; Price, G. Magnetically processed carbon nanotube/epoxy nanocomposites: morphology, thermal, and mechanical properties. *Polymer* **2010**, *51*, 1614−1620.
(26) Sahoo, N. G.; Sravendra, R.; Jae, W. C. Polymer nanocomposites based on functionalized carbon nanotubes. *Prog. Polym. Sci.* **2010**, *35*, 837−867.

https://doi.org/10.1021/acsomega.1c05606
ACS Omega 2022, 7, 1347−1356